POLITECNICO DI TORINO
Repository ISTITUZIONALE

Unveiling the Dependence between Hydroxyl Radical Generation and Performance of Fenton Systems with Complexed Iron

Original
Unveiling the Dependence between Hydroxyl Radical Generation and Performance of Fenton Systems with Complexed Iron / Garcia-Negueroles, P.; Garcia-Ballesteros, S.; Amat, A. M.; Laurenti, E.; Arques, A.; Santos-Juanes, L.. - In: ACS OMEGA. - ISSN 2470-1343. - 4:26(2019), pp. 21698-21703. [10.1021/acsomega.9b02241]

Availability:
This version is available at: 11583/2993772 since: 2024-10-28T11:03:32Z

Publisher:
American Chemical Society ACS

Published
DOI:10.1021/acsomega.9b02241

Terms of use:

This article is made available under terms and conditions as specified in the corresponding bibliographic description in the repository

Publisher copyright

(Article begins on next page)

06 May 2026

Paper FUSENGDES-D-17-00546

Divertor currents optimization procedure for JET-ILW high flux expansion experiments

G.Calabrò et al.

Highlights

Author's proposal:

- ***High flux expansion configuration obtained by divertor currents optimization at JET***
- ***Divertor magnetic topology characterized by the presence of two nearby field nulls***
- ***Flux expansion effects on total power radiation for H-mode nitrogen seeded discharges***

Reply to reviewers

Paper FUSENGDES-D-17-00546
G. Calabrò et al., "Divertor currents optimization procedure for JET-ILW high flux expansion experiments"

Reply to reviewer#1

Reviewer's general comment: The present manuscript discusses an optimization procedure to increase divertor flux expansion on the JET tokamak within machine constraints and presents some preliminary experimental results. In my opinion, the manuscript fits into the scope of Fusion Engineering and Design. However, a number of improvements and adjustments are required before I can recommend it for publication.

Authors' reply:

We thank the reviewer for the useful comments. We found them extremely helpful in the revision process. We will explicate how we have addressed each of the concerns in the following. First, we will give detailed responses to your comments. Then, in light of your comments, we have made some changes to the text. We sincerely hope that we have addressed all the reviewer concerns in a satisfactory manner.

Reviewer's comment #1

The authors stress the possible advantages of strong flux expansion and flaring. Recently, a number of benefits of this configuration have been demonstrated experimentally on TCV (Theiler et al., Nucl. Fusion 57 (2017) 072008, showing deeper detachment and a reduction in the radiation location sensitivity to core density with increasing flux expansion and flaring) and DIII-D (Covele et al., Nucl. Fusion 57 (2017) 086017, showing that increasing flux expansion and flaring allow for detachment at lower density and higher pedestal pressure). The authors should refer to these results to emphasis the interest in these configurations. This could be done in the introduction after the sentence ending as "?causing flared field lines there, which spreads the heat over a larger area and increases the line connection length".

Authors' reply:

We have added reference to the suggested papers in the new version of the paper. Indeed, we have modified the Introduction as following:

➔ *Introduction: "…An approach to handle the heat exhaust power is to use alternative magnetic configurations, such as Snowflake Divertor (SF) [3] and recently described divertor with a strong flux flaring in a single divertor leg [4, 5]. Such a configuration places the second x-point near the plate, causing flared field lines in that region which spread the heat load over a larger area and increase the line connection length. Recently, a number of benefits of High Flux Expansion (HFE) configurations have been experimentally demonstrated on TCV [Theiler et al., Nucl. Fusion 57 (2017) 072008] and DIII-D [Covele et al., Nucl. Fusion 57 (2017) 086017]. On the former, HFE configuration showed deeper detachment and a reduction of the radiation location sensitivity with respect to the plasma core density, with increasing flux expansion and flaring; on the latter, it showed that increasing flux expansion and flaring allow for detachment at lower density and higher pedestal pressure."*

Reviewer's comment #2

In the abstract and at other places (e.g. line 6 of the introduction) the authors state that HFE configurations are promising"? thanks to their feature to flare the heat loads yield by the Scrape-Off Layer (SOL) on a wider region ?" However, heat flux spreading over a larger area can also be achieved by tilting the divertor plates in the poloidal plane (this is well explained for example in the paper by Theiler et al. mentioned above). Therefore, the above statement by the authors is misleading. In an existing machine, where the wall geometry is fixed, the statement might be justified. However, when designing a new machine, the wall geometry will certainly be optimized the have angles as low as technically possible between the total magnetic field and divertor plate. Therefore, please motivate better the interest in HFE configurations (see also point 1)).

Authors' reply:
We agree with the Reviewer that statement on benefits of HFE configuration at JET would need more support and additional justification.
HFE experiments at JET, existing machine with fixed geometry wall, have been motivated by the aim to study the effects of flux expansion variation, mainly at the xpoint location than at targets, on radiation fraction and divertor radiated power re-distribution. In the past at JET, with the MkI divertor, a systematic study of the influence of X-point height and poloidal flux expansion has been set up [C. Lowry , et al. , Divertor configuration studies on jet, J. Nucl. Mater. 241–243 (1997) 438–443, A. Loarte, et al., Plasma detachment in JET mark I divertor experiments, Nucl. Fusion 38 (3) (1998) 331–371] showing minor differences in the radiation distribution, whereas in [R. Pitts, et al., Divertor geometry effects on detachment in TCV, J. Nucl. Mater. 290–293 (2001) 940–946, doi: 10.1016/S0022-3115(00)00461-X] experiments and simulations have shown enhancement of detachment as the flux expansion was increased. More recently at JET, equipped with the ITER-like Wall (ILW), radiative seeded scenarios have been studied and only a maximum radiation fraction 75% has been achieved [M. Wischmeier, et al., Impurity Seeding on JET to Achieve Power Plant like Divertor Conditions, presented at 25th FEC – IAEA Conference, St Petersburg (2014), *http://www-naweb.iaea.org/napc/physics/FEC/FEC2014/fec2014-slides/94_EX72.pdf]. However, high flux expansion configuration are predicted to increase the radiation in the vicinity of the X-point and have a ionization front extending further in the SOL than the LFE equilibrium, as discussed in [B. Viola et al., Nuclear Materials and Energy, 12 (2017) 786-790]. Finally, HFE cases do seem to offer a benefit in reducing the nitrogen concentration needed to obtain a given radiated power level [B. Viola et al., Nuclear Materials and Energy, 12 (2017) 786-790].*
However, only a brief discussion on experimental effect of flux expansion on radiation fraction will be given in the proposed paper because a contribution to the coming IAEA 2018 conference is already planned, mainly focused on the physical aspects of the HFE experiments.

Additional Authors' reply:
Consequently, we have modified the Introduction as following:
➔ *Introduction: "…In the past at JET, with the MkI divertor, a systematic study of the influence of x-point height and poloidal flux expansion has been set up [C. Lowry , et al. , Divertor configuration studies on jet, J. Nucl. Mater. 241–243 (1997) 438–443, A. Loarte, et al., Plasma detachment in JET mark i divertor experiments, Nucl. Fusion 38 (3) (1998) 331–371] showing minor differences in the radiation distribution, whereas in [R. Pitts, et al., Divertor geometry effects on detachment in TCV, J. Nucl. Mater. 290–293 (2001) 940–946, doi: 10.1016/S0022-3115(00)00461-X], experiments and simulations have shown an enhancement of detachment as the flux expansion was increased. More recently at JET, equipped with ITER-like Wall [E. Joffrin, et al., Nuclear Fusion, 54 (2014) 013011], radiative seeded scenarios have been studied and only a maximum 75% radiation fraction has been achieved [M. Wischmeier, et al., Impurity Seeding on JET to Achieve Power Plant like Divertor Conditions, presented at 25th FEC – IAEA Conference, St Petersburg (2014), http://www-naweb.iaea.org/napc/physics/FEC/FEC2014/fec2014-slides/94_EX72.pdf]. However, recent predictive studies [B. Viola et al., Nuclear Materials and Energy, 12 (2017) 786-790] have shown that HFE configurations increase the radiation in the proximity of the x-point and have an ionization front extending further in the Scrape-Off Layer (SOL) than in the Low Flux Expansion (LFE) case. In addition, HFE cases do seem to offer a benefit in reducing the nitrogen concentration needed to obtain a given radiated power level [16]. Here, we will discuss the modelling, creation and control of HFE configurations at JET–ILW, characterized by the presence of two nearby poloidal field nulls in the divertor region, aimed to study the effects of flux expansion variation on radiation fraction and radiated power re-distribution."*

Additional Authors' reply:
In addition, we have substantially revised the "Abstract" as following:
➔ *Abstract: "This paper deals with a divertor coil currents optimized procedure to design High Flux Expansion (HFE) configurations in the JET tokamak aimed to study the effects of flux expansion variation on the radiation fraction and radiated power re-distribution. A number of benefits of HFE configuration have been experimentally demonstrated on TCV, EAST, NSTX and DIII-D tokamaks and are under investigation for*

next generation devices, as DEMO and DTT. The procedure proposed here exploits the linearized relation between the plasma-wall gaps and the Poloidal Field (PF) coil currents. Once the linearized model is provided by means of CREATE-NL code, the divertor coils currents are calculated using a constrained quadratic programming optimization procedure, in order to achieve HFE configuration. HFE configurations have been experimentally realized both in ohmic and heated plasma with and without nitrogen seeding. Preliminary results on the effects of the flux expansion variation on total power radiation increase will be also briefly discussed."

Reviewer's comment #3

I don't understand why the matrix H and the vector f in equation (1) are necessarily the identity matrix and the zero vector. I understood that the authors first introduce the general optimization procedure, equation (1), and later adapt it to their specific problem, equation (2). If so, in equation (1), the matrix H and the vector f can be more general, correct? Otherwise, I don't understand why the authors even introduce H and f.

***Authors' reply**:*

We agree with the Reviewer. The text has been adapted, as following, in order to make this point clear:

➔ *Section 2: "…Once the linearized model is provided by means of CREATE-NL code, the divertor coils current needed to achieve the HFE configuration are calculated by means of a constrained quadratic programming optimization procedure [Coleman, T.F. and Y. Li, "A Reflective Newton Method for Minimizing a Quadratic Function Subject to Bounds on Some of the Variables," SIAM Journal on Optimization, Vol. 6, Number 4, pp. 1040–1058, 1996, Gould, N. and P. L. Toint. "Pre-processing for quadratic programming."* Math. Programming*, Series B, Vol. 100, pp. 95–132, 2004], generally stated as follows:*

$$\min_{\underline{x}} \frac{1}{2}\underline{x}^T \underline{\underline{H}}\underline{x} + \underline{f}^T \underline{x} \text{ subject to: } \begin{cases} \underline{\underline{A}} \cdot \underline{x} = \underline{b} \\ \underline{l_b} \le \underline{x} \le \underline{u_b} \end{cases} \qquad (1)$$

where the symmetric matrix $\underline{\underline{H}}$ *represents the quadratic term, the vector* $\underline{f}$ *is the linear term, whilst the matrix* $\underline{\underline{A}}$ *and the vector* $\underline{b}$ *represent respectively the linear coefficients and the constant in the constraint of Eq. (1). At last, vectors* $\underline{l_b}$ *and* $\underline{u_b}$ *represent respectively the lower and upper bounds elementwise in (1). Once matrix* $\underline{\underline{H}}$ *and vector* $\underline{f}$ *are set up respectively as identity matrix and zero vector, finding a minimum for a problem specified by Eq. (1) turns into minimizing the Euclidean norm of the unknown vector* $\underline{x}$ *and guaranteeing the convexity of the objective function as well as the uniqueness of the optimization problem solution. Hence, Eq. (1) is adapted to the specific problem of achieving HFE plasma configurations while minimizing currents variation* $\underline{\Delta I}$ *in the PF coils subject to technological restrictions. Indeed, the vector* $\underline{x} = \underline{\Delta I}$ *must accomplish specific constraints, modelled by means of the linear equality constraints set thanks to the adopted linearized model: plasma shape and total plasma current are requested to be kept unchanged, whilst flux expansion is increased. Moreover* $\underline{x}$ *must be bounded according to the current restrictions on PF coil power supplies. Consequently, the constrained quadratic programming optimization procedure turns into the following problem:*

$$\min \left\| \underline{\Delta I} \right\|_2 \text{ subject to: } \begin{cases} \underline{\underline{A}}_{gaps-I} \cdot \underline{\Delta I} = \underline{0} \\ \underline{L}^T_{plasma-I} \cdot \underline{\Delta I} = 0 \\ \underline{\underline{A}}_{FExp-I} \cdot \underline{\Delta I} = \underline{\delta}_{FExp} \\ \underline{I}_{\min} - \underline{I}_0 \le \underline{\Delta I} \le \underline{I}_{\max} - \underline{I}_0 \end{cases} \qquad (2)$$

where:

$\underline{\underline{A}}_{gaps-I}$ *represents the linearized relationship between the* I_{PF} *currents and the plasma-wall gaps to be controlled (the first constraint states that the variation of* I_{PF} *currents does not affect the plasma-wall gaps); the following five gaps have been specifically considered [Marco Ariola, Alfredo Pironti,*

Magnetic Control of Tokamak Plasmas, 2008 Springer-Verlag London Limited, DOI 10.1007/978-1-84800-324-8] in our analyses: Radial Outer Gap (ROG), Radial Inner Gap (RIG), Top Gap (TOG), R coordinate of Outer Strike Point (RSOGB) and Z coordinate of Inner Strike Point (ZSIGB);

$\underline{L}_{plasma-I}$ *represents the mutual inductance vector between the plasma and the active coils (the second constraint states that the variation of* I_{PF} *currents does not affect the total plasma current);*

$\underline{\underline{A}}_{FExp-I}$ *represents the linearized relationship between the* I_{PF} *currents and the magnetic flux expansion (the third constraint states that the variation of* I_{PF} *currents changes the flux expansion, here assumed to be the Full flux Expansion* $f_{x,t}$ *of the SOL boundary with decay length* λ_q *= 2mm, according to* $\underline{\delta}_{FExp}$ *).*

$\underline{I}_0$ *is the* I_{PF} *currents vector in the reference equilibrium (the last constraint bounds the currents flowing into the* I_{PF} *currents according to the technological restrictions of each power supply, in terms of minimum and maximum attainable values; specifically, the following lower and upper bounds have been considered for each of the divertor coil:* $I_{D1}\{0,19kA\}$, $I_{D2}\{0,37kA\}$, $I_{D3}\{0,37kA\}$, $I_{D4}\{-18kA,0\}$.

Reviewer's comment #4

Page 4: The definition of the different flux expansions is not entirely clear. What is the SOL boundary? Is it the flux surface at one e-folding length away from the separatrix? If so, please state this clearly and already mention here what is assumed for lambda_q. Also, the authors say that the flux expansion is the DISTANCE between two flux surfaces. However, flux expansion is usually not a length but a ratio of two lengths. This should be clarified. The definition of the flux expansion at the x-point is also not very clear. For better illustration, the authors could maybe add some information in figure 2a?

***Authors' reply**:*

We agree with the Reviewer. The text and Figures 2 have been adapted, as following, in order to make this point clear. The definition of the flux expansion has been moved to Section 2, where we introduce the optimization procedure, as following:

➔ *Section 2: "The magnetic geometry in the divertor can be modified by changing the flux expansion at the target* $f_{x,t} = dr_{target}/\lambda_q$ *[17]:* dr_{target} *is the distance along the First Wall boundary between the inner (or outer) strike points of the separatrix and of the SOL boundary (i.e. the flux surface at one e-folding length power decay* λ_q *away from the separatrix);* λ_q *is the SOL width on the outer plane containing the plasma centroid. It should be noted that in JET, due to the location and geometry of the target plates, the inner and outer strike points of SOL boundary might be in a different position when moving from LFE to HFE configuration. In order to avoid this issue we consider the Full Flux Expansion at the target as the ratio between* $dr_{target,tube}$ *(i.e. the poloidal expansion of the magnetic flux tube at the target) and the SOL width (see Fig.2a in Section 3). In addition, we consider the flux expansion at x-point as* $f_{x,xp} = dr_{xpoint}/\lambda_q$*, where* dr_{xpoint} *is the Euclidian distance between the x-point and the SOL boundary along the horizontal line inward and outward the x-point height (see Fig.2a). For sake of consistency, the same rectangular grid has been used when scanning the SOL width on the plane containing the plasma centroid. Specifically, SOL width* λ_q *of 2, 5 and 10 mm have been considered."*

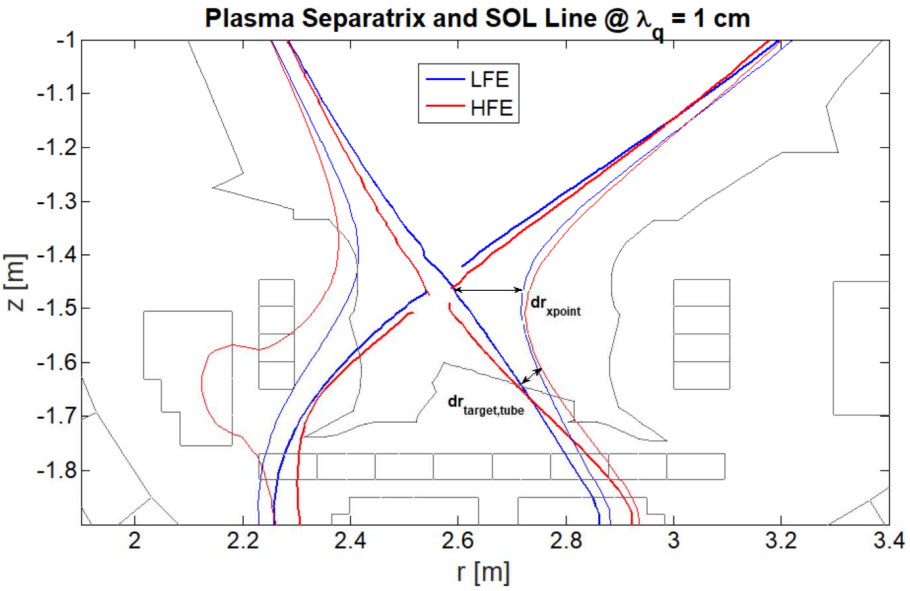

(New) **Fig.2a**: Plasma separatrix and SOL flux surface with λ_q=1cm, for both LFE (discharge #90541 at 61s) and HFE (discharge #90541 at 65s) configurations.

Additional Authors' reply:

Consequently we have modified the initial part of Section 3 as following:

➔ *Section 3: "Initial HFE ohmic and nitrogen seeded H-mode discharges, at plasma current I_P=1.8MA have been successfully achieved at JET – ILW. Table I reports the values of both $f_{x,t}$ and $f_{x,xp}$, considering a SOL width of λ_q=2mm, for the ohmic discharge #90541 when moving from LFE to HFE configuration. Plasma separatrix and flux surface at λ_q=1cm for both LFE and HFE configurations are shown in Fig. 2a. Plasma separatrix and poloidal magnetic field module iso-lines, with B_P varying from 0-0.05T, are shown for both LFE (Fig. 2b) and HFE (Fig.2c) configurations. It should be noted that the magnetic field flatness region is increased for HFE configuration thanks to the presence of a second x-point…"*

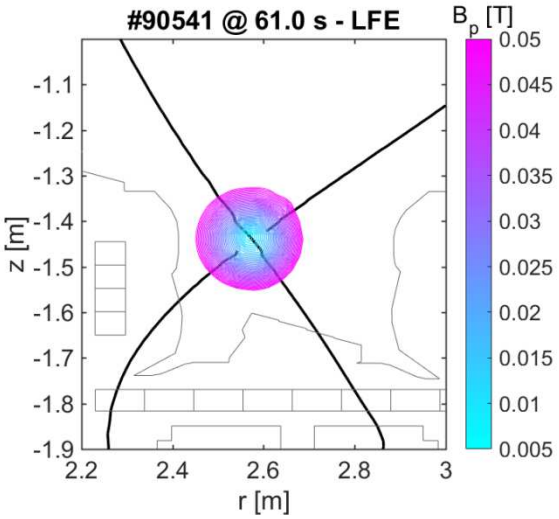

(New) Fig.2b. *Plasma separatrix and poloidal magnetic field module iso-lines, with B_P varying from 0-0.05T, are shown for LFE configuration.*

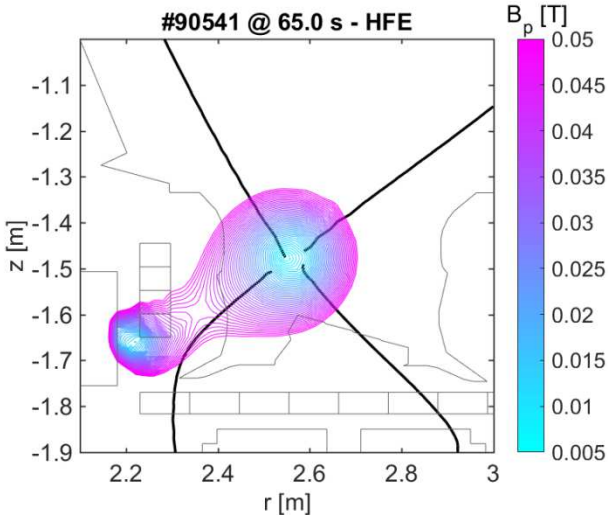

(New) Fig.2c. *Plasma separatrix and poloidal magnetic field module iso-lines, with B_P varying from 0-0.05T, are shown for LFE configuration.*

Reviewer's comment #5

Still on page 4: the authors mention a distance d_x1-x2. It should be mentioned that this is a normalized length. And if the authors could define d_x1-x2 here instead of referring to other papers, this would help the reader a lot.

Authors' reply:

We thank the Reviewer for the useful suggestions. The text and Figure 3 have been adapted, as following, in order to make this point clear. By the way, previous Figure 3 now becomes Figure 4 in the new version of the paper. Indeed, a new Figure (the new Figure 3) has been introduced in the new version of the paper, in order to judge the gaps and total plasma current variation due to the optimization procedure for HFE experimental discharge compared to the LFE reference one.
Here the modification on the text and the new Figure 4:
➔ *Section 3: "…The distance between the two null-points, i.e the proximity to the exact SF [D.D. Ryutov, V.A. Soukhanovskii, Physics of Plasmas 22, 110901 (2015), G. Calabrò, et al., Nuclear Fusion 55 (8), 083005 (2015)], is parametrized here by the dimensionless factor σ = D/a, where D is the null-points separation distance and a is the plasma minor radius. SF like configuration corresponds to σ close to zero. The mutual position of the primary and secondary null-points determines the local geometry of the null region and hence the properties of the divertor. Experimental values of the flux expansion at the inner and outer x-point $f_{x,xp}$ vs. SF proximity parameter σ are shown in Fig. 4 for JET–ILW discharges. Both inner and outer $f_{x,xp}$ increase when moving from LFE (σ=1) to HFE configuration (0.25<σ<0.45). The maximum flux expansion increase has been obtained for the discharge #92086 by relaxing the plasma distance to the inner wall. It should be noted that this configuration cannot be used in H-mode discharges because of the limitations on the permitted operational plasma-wall distance for heated plasmas."*

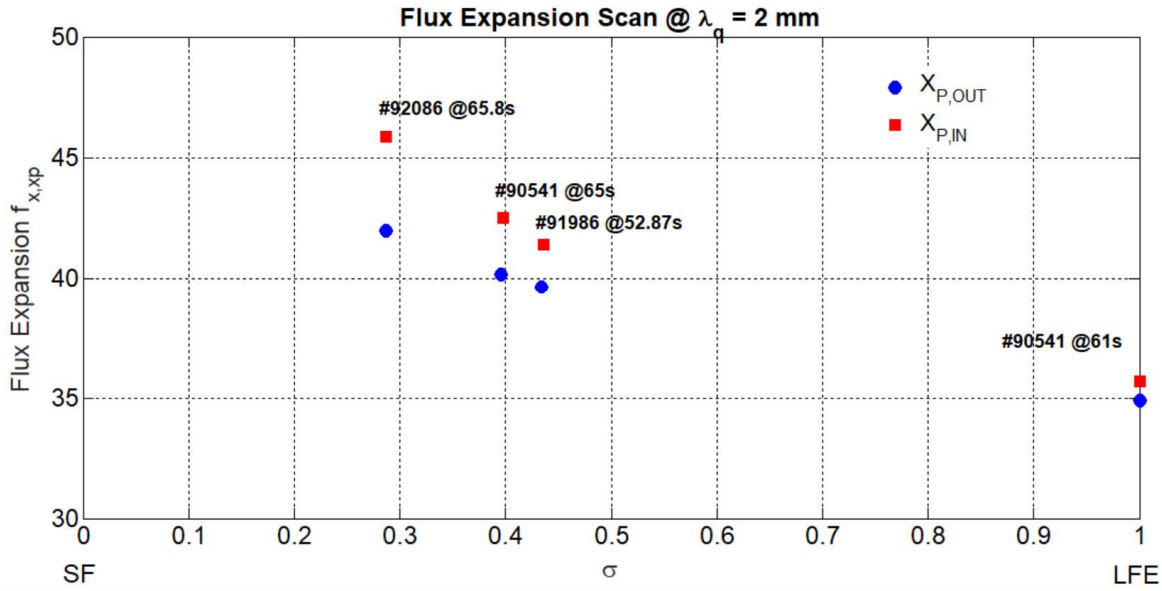

(New) Figure 4. Experimental values of the flux expansion at the inner and outer x-point $f_{x,xp}$ vs. SF proximity parameter σ. Both inner and outer $f_{x,xp}$ increase when moving from LFE configuration (σ=1) to HFE configuration (0.25<σ<0.45), characterized by the presence of 2-nearby poloidal field nulls.

Reviewer's comment #6

In figure 3, the flux expansion for X_p,in is always larger than X_p,out. The opposite is the case in Table I. Please clarify.

***Authors' reply**:*

We thank the Reviewer for the comment. Table I has been corrected as following:

Table I. Flux expansion on inner and outer x-point and targets. A SOL width of λ_q = 2 mm has been considered, accordingly with the length-decay of the thermal power in the SOL in JET tokamak [T. Eich, et al., PRL 107, 215001 (2011)]

	$f_{x,xp/IN}$	$f_{x,xp/OUT}$	$f_{x,t/IN}$	$f_{x,t/OUT}$
HFE JPN #90541 @ 65 s I_{D1} = 6.36 kA, I_{D2} = 5.04 kA, I_{D3} = 11.19 kA, I_{D4} = 0 kA	*42.52*	*40.44*	*12.63*	*5.96*

LFE JPN #90541 @ 61 s I_{D1} = 1.51 kA, I_{D2} = 13.91 kA, I_{D3} = 6.41 kA, I_{D4} = -4.34 kA	*35.66*	*34.39*	*6.20*	*4.08*

Reviewer's comment #7

Do the flux surfaces shown in figure 2a) for the LFE and HFE cases correspond to the same distances in the SOL?

Authors' reply:

Flux surfaces shown in (new) figure 2a) for the LFE and HFE cases correspond to the same distances in the SOL (i.e. λ_q = 1cm) as discussed in Author's reply to Reviewer's comment #4.

Reviewer's comment #8

Similarly, for the contours shown in figure 2b and 2c: Do the magenta lines in the two plots correspond to the same values of the poloidal flux? It seems not to be the case, as 2b shots 7 contours and 2c shows 8 contours. For a better comparison, I think it would be good to use corresponding contours in both plots.

Authors' reply:

We thank the Reviewer for the comment. We have already modified, for a better explanation, Fig.2b and 2c as discussed in Author's reply to Reviewer's comment #4. Magenta lines were the magnetic field module iso-lines corresponding, in both plots 2b and 2c, to the same values of the poloidal magnetic field B_P [0,0.05T]. The magnetic field module iso-lines are added to the plasma separatrix to highlight the increase of the magnetic field flatness region for the HFE configuration. Indeed, the position of secondary x_2 null point relative to x_1 one, as previously discussed, determines the local geometry of the null region and hence the properties of the divertor. In addition, we have also removed the text "x1" and "x2" from Fig.2b and 2c. Indeed, the "x1" text was covering the smallest magnetic field iso-line as it makes confusion to the reader.

Reviewer's comment #9

For better visibility, it would be good to zoom in on figure 1

Authors' reply:

We thank the Reviewer for the comment. Fig.1 has been modified in the new version of the paper, as following:

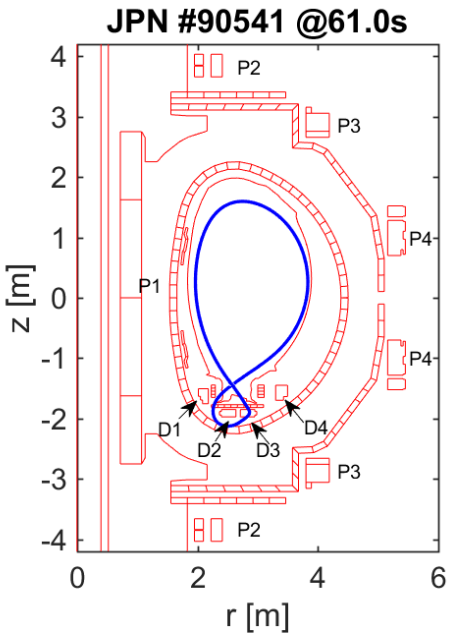

(New) Figure 1. Cross section of the JET tokamak. The plasma boundary of JET discharge #90541 at 61s is shown in blue. The poloidal coils (P1–P4 and D1–D4) and the toroidal coils, which surround the plasma ring, produce the required magnetic field for plasma confinement. Here, the D coils current are used on the optimization procedure in order to locally modify the magnetic topology in the divertor region.

Reviewer's comment #10

It would be good if the authors could improve a bit the English and correct typos. Below a few examples (but please correct the entire text):

a) Abstract: "might present a well promising" -> "might present a promising"
b) Introduction, line 8: "itself and its and its" -> "itself and its"
c) Sentence near the bottom of page 2: "Minimize a convective objective function" appears twice in the same sentence. Please correct this sentence.
d) References [2] and [12] are identical
e) Conclusions: "controlling a two" -> "controlling two"

***Authors' reply**:*

We thank the Reviewer for the comment and for the suggestions to improve English and correct typos. The entire text has been improved in terms of English language and the typos have been corrected.

Reply to reviewers

Paper FUSENGDES-D-17-00546
G. Calabrò et al., "Divertor currents optimization procedure for JET-ILW high flux expansion experiments"

Reply to reviewer#2

Reviewer's general comment: The paper is of good quality and suitable for the publication in Fusion Engineering and design.

Authors' reply:

We thank the reviewer for the useful comments. We found them extremely helpful in the revision process. We will explicate how we have addressed each of the concerns in the following. First, we will give detailed responses to your comments. Then, in light of your comments, we have made some changes to the text. We sincerely hope that we have addressed all the reviewer concerns in a satisfactory manner.

Reviewer's comment #1:

The authors should add some details about the formulation and solution of the optimization problem.

Authors' reply: We thank the Reviewer for the comment. *The text and Figures have been adapted in the new version of the paper, as following, in order to make this point clear.*

a) How many gaps were used for keeping fixed the plasma boundary?

Authors' reply: *the following five gaps have been specifically considered [Marco Ariola, Alfredo Pironti, Magnetic Control of Tokamak Plasmas, 2008 Springer-Verlag London Limited, DOI 10.1007/978-1-84800-324-8]: Radial Outer Gap (ROG), inner radial gap (RIG), Top Gap (TOG), R coordinate of Outer Strike Point (RSOGB) and Z coordinate of Inner Strike Point (ZSIGB). However, we include here (not presented in the paper) a Figure to better explain the gaps used in the simulations (Figure 9.2 of the abovementioned book]:*

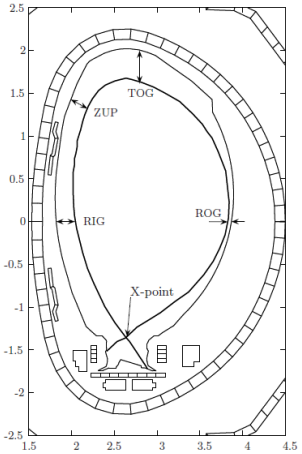

Figure: Some JET gaps. The figure shows some of the gaps defined for the JET control system:

- RIG is the Radial Inner Gap,
- TOG is the Top Gap,
- and ROG is the Radial Outer Gap.

A gap is the distance between the plasma surface and the first wall, measured along a given direction

b) In the expression (1), lb and ub parameters should be defined.

Authors' reply: *vectors l_b and u_b represent respectively the lower and upper bounds elementwise in Expression (1). However, we agree with the Reviewer to add further details about the formulation and solution of the optimization problem. Indeed, the text has been adapted, as following, in order to make this point clear:*

➔ *Section 2: "…Once the linearized model is provided by means of CREATE-NL code, the divertor coils current needed to achieve the HFE configuration are calculated by means of a constrained quadratic programming optimization procedure [Coleman, T.F. and Y. Li, "A Reflective Newton Method for Minimizing a Quadratic Function Subject to Bounds on Some of the Variables," SIAM Journal on Optimization, Vol. 6,*

Number 4, pp. 1040–1058, 1996, Gould, N. and P. L. Toint. "Pre-processing for quadratic programming." Math. Programming*, Series B, Vol. 100, pp. 95–132, 2004], generally stated as follows:*

$$\min_{\underline{x}} \frac{1}{2}\underline{x}^T \underline{\underline{H}}\underline{x} + \underline{f}^T \underline{x} \text{ subject to: } \begin{cases} \underline{\underline{A}} \cdot \underline{x} = \underline{b} \\ \underline{l_b} \le \underline{x} \le \underline{u_b} \end{cases} \quad (1)$$

where the symmetric matrix $\underline{\underline{H}}$ *represents the quadratic term, the vector* $\underline{f}$ *is the linear term, whilst the matrix* $\underline{\underline{A}}$ *and the vector* $\underline{b}$ *represent respectively the linear coefficients and the constant in the constraint of Eq. (1). At last, vectors* $\underline{l_b}$ *and* $\underline{u_b}$ *represent respectively the lower and upper bounds elementwise in (1). Once matrix* $\underline{\underline{H}}$ *and vector* $\underline{f}$ *are set up respectively as identity matrix and zero vector, finding a minimum for a problem specified by Eq. (1) turns into minimizing the Euclidean norm of the unknown vector* $\underline{x}$ *and guaranteeing the convexity of the objective function as well as the uniqueness of the optimization problem solution. Hence, Eq. (1) is adapted to the specific problem of achieving HFE plasma configurations while minimizing currents variation* $\underline{\Delta I}$ *in the PF coils subject to technological restrictions. Indeed, the vector* $\underline{x} = \underline{\Delta I}$ *must accomplish specific constraints, modelled by means of the linear equality constraints set thanks to the adopted linearized model: plasma shape and total plasma current are requested to be kept unchanged, whilst flux expansion is increased. Moreover* $\underline{x}$ *must be bounded according to the current restrictions on PF coil power supplies. Consequently, the constrained quadratic programming optimization procedure turns into the following problem:*

$$\min \left\| \underline{\Delta I} \right\|_2 \text{ subject to: } \begin{cases} \underline{\underline{A}}_{gaps-1} \cdot \underline{\Delta I} = \underline{0} \\ \underline{L}^T_{plasma-1} \cdot \underline{\Delta I} = 0 \\ \underline{\underline{A}}_{FExp-1} \cdot \underline{\Delta I} = \underline{\delta}_{FExp} \\ \underline{I}_{\min} - \underline{I}_0 \le \underline{\Delta I} \le \underline{I}_{\max} - \underline{I}_0 \end{cases} \quad (2)$$

where:

$\underline{\underline{A}}_{gaps-I}$ *represents the linearized relationship between the* I_{PF} *currents and the plasma-wall gaps to be controlled (the first constraint states that the variation of* I_{PF} *currents does not affect the plasma-wall gaps); the following five gaps have been specifically considered [Marco Ariola, Alfredo Pironti, Magnetic Control of Tokamak Plasmas, 2008 Springer-Verlag London Limited, DOI 10.1007/978-1-84800-324-8] in our analyses: Radial Outer Gap (ROG), Radial Inner Gap (RIG), Top Gap (TOG), R coordinate of Outer Strike Point (RSOGB) and Z coordinate of Inner Strike Point (ZSIGB);*

$\underline{L}_{plasma-I}$ *represents the mutual inductance vector between the plasma and the active coils (the second constraint states that the variation of* I_{PF} *currents does not affect the total plasma current);*

$\underline{\underline{A}}_{FExp-I}$ *represents the linearized relationship between the* I_{PF} *currents and the magnetic flux expansion (the third constraint states that the variation of* I_{PF} *currents changes the flux expansion, here assumed to be the Full flux Expansion* $f_{x,t}$ *of the SOL boundary with decay length* λ_q *= 2mm, according to* $\underline{\delta}_{FExp}$ *).*

$\underline{I}_0$ *is the* I_{PF} *currents vector in the reference equilibrium (the last constraint bounds the currents flowing into the* I_{PF} *currents according to the technological restrictions of each power supply, in terms of minimum and maximum attainable values; specifically, the following lower and upper bounds have been considered for each of the divertor coil:* I_{D1}*{0,19kA }*, I_{D2}*{0,37kA }*, I_{D3}*{0,37kA }*, I_{D4}*{-18kA,0 }.*

c) The "flux expansion" should be defined before of the paragraph 3.

Authors' reply: We agree with the Reviewer, we moved the flux expansion definition to Section 2. More details will be given later in this document .

d) The "flux expansion on the inner/outer target" definition should be reviewed:
Authors' reply: We agree with the Reviewer, we have given more details on the flux expansion definitions. All the aforementioned further details will be given later in this document.

e) The SOL boundary should be defined.
Authors' reply: *Scrape-Off Layer (SOL) boundary is defined as the flux surface at one e-folding length λ_q away from the separatrix. Specifically, a SOL width (or e-folding length) λ_q of 2, 5 and 10mm on the outer plane where the plasma centroid is located, have been considered in our calculations.*

f) The distance between separatrix and divertor target depends on the poloidal position; If the strike points of the SOL boundary with the inner and outer targets differ in the LFE and HFE configurations, the measure of the flux expansion by the given definition appears to be of a loose consistency. Moreover, in chap. 3, Table I, flux expansion is reported as an a-dimensional quantity!
Authors' reply: *We agree with the Reviewer's comment. The text and Figures 2 have been adapted, as following, in order to make this point clear. The definition of the flux expansion has been moved to Section 2, where we introduce the optimization procedure, as following:*

➔ *"The magnetic geometry in the divertor can be modified by changing the flux expansion at the target $f_{x,t} = dr_{target}/\lambda_q$ [17]: dr_{target} is the distance along the First Wall boundary between the inner (or outer) strike points of the separatrix and of the SOL boundary (i.e. the flux surface at one e-folding length power decay λ_q away from the separatrix); λ_q is the SOL width on the outer plane containing the plasma centroid. It should be noted that in JET, due to the location and geometry of the target plates, the inner and outer strike points of SOL boundary might be in a different position when moving from LFE to HFE configuration. In order to avoid this issue we consider the Full Flux Expansion at the target as the ratio between $dr_{target,tube}$ (i.e. the poloidal expansion of the magnetic flux tube at the target) and the SOL width (see Fig.2a in Section 3). In addition, we consider the flux expansion at x-point as $f_{x,xp} = dr_{xpoint}/\lambda_q$, where dr_{xpoint} is the Euclidian distance between the x-point and the SOL boundary along the horizontal line inward and outward the x-point height (see Fig.2a). For sake of consistency, the same rectangular grid has been used when scanning the SOL width on the plane containing the plasma centroid. Specifically, SOL width λ_q of 2, 5 and 10 mm have been considered."*

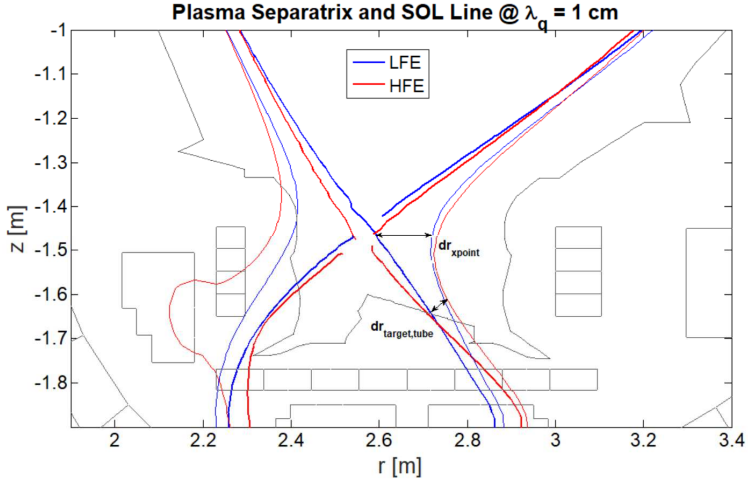

(New) **Fig.2a**: Plasma separatrix and SOL flux surface with λ_q=1cm, for both LFE (discharge #90541 at 61s) and HFE (discharge #90541 at 65s) configurations.

g) Were the constraints imposed by the penalty method? What values were used for the penalty coefficients?

***Authors' reply**: the optimization procedure used here is based on a reflective newton* method for minimizing a quadratic function subject to bounds on some of the variables. The Authors have used the MatLab function "quadprod". Further details are given in the following references:

I. https://it.mathworks.com/help/optim/ug/quadprog.html
II. *Coleman, T.F. and Y. Li, "A Reflective Newton Method for Minimizing a Quadratic Function Subject to Bounds on Some of the Variables," SIAM Journal on Optimization, Vol. 6, Number 4, pp. 1040–1058, 1996;*
III. Gould, N. and P. L. Toint. "Pre-processing for quadratic programming." *Math. Programming*, Series B, Vol. 100, pp. 95–132, 2004.

h) The gaps and plasma current variation due to the optimization procedure should be specified.

***Authors' reply**: we thank the Reviewer for the useful suggestions. A new Figure (named Fig. 3, shown on the next Author's reply) has been added in the new version of the paper in order to judge the gaps and total plasma current variation due to the optimization procedure for HFE experimental discharge compared to the LFE reference one.*

i) How much increases the power of the divertor coils for the HFE optimized configuration with respect to the LFE reference case?

***Authors' reply**: we thank the Reviewer for the useful comment. In the same new Figure 3 (shown both here and in the new version of the paper), we have added the divertor coil currents values due to the optimization procedure for HFE experimental discharge compared to the LFE reference one. All the divertor coil currents are kept well below the power supply limits. However, the main difference between the HFE and LFE configuration in terms of power of the divertor coil is related to I_{D4} current, that is requested to be at zero value. Indeed, in these experiments, the maximum attainable flux expansion has been mainly limited to the polarity on D4 coil (positive for I_{D1},..I_{D3} and negative for I_{D4}). A further increase on the both outer x-point and* target *flux expansion, that consequently it is translated into the movement of the secondary (x2) null on the outer region, could be obtained changing the polarity on D4 coil.*

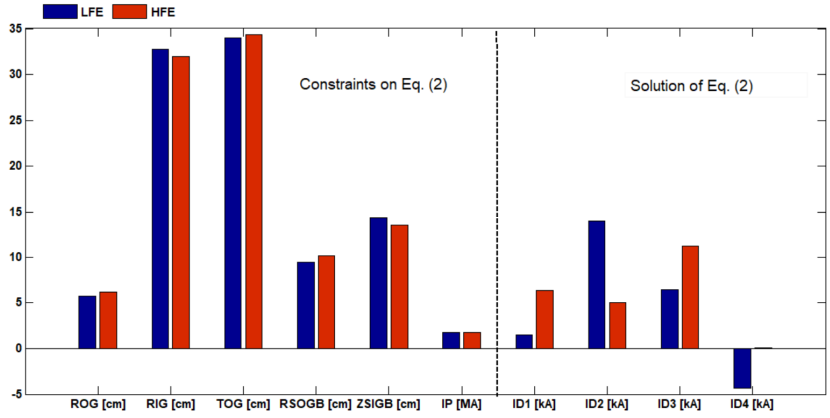

(New) **Figure 3**: Comparison between experimental LFE (blue color) and HFE configuration (red color) in terms of constraints imposed in Eq. (2), i.e. the five gaps (RIG, ROG, TOG, RSOGB and ZSIGB) and plasma current I_P to be kept almost unchanged, and divertor coil currents, i.e. the outputs of the optimization procedure, to be varied in order to increase the flux expansion. The maximum attainable flux expansion has been mainly limited to the polarity on D4 coil

Reviewer's comment #2: In my opinion, the space domain where the second null should be searched by the optimization problem depends on the selected approach for handling the heat exhaust power. If the objective is to increase the wetted divertor surface, the additional null point should be placed near to the divertor (vertical) targets. Alternatively if the heat power would be dissipated by a surface (hot)-surface(cold) radiation mechanism, as the authors suggest, the optimization problem target should be the maximization of both radiating (hot) and radiated (cold) surfaces. The radiating surface can be increased by HFE, as suggested by the authors and evidenced in Figure 2C. On the other hand, the maximization of the radiated surface could be obtained by the collocation of the additional null point in the spatial position where the sight angle of the reactor passive components (from the radiating region) is maximized. This target could be pursued by delimiting opportunely the space region where the additional null point would be searched. On this respect, the position of the second null shown in fig. 2c doesn't look be optimal because the radiating region faces directly the plasma region.

***Authors' reply**:*

We agree with the Reviewer for the comments. Indeed, the space domain where the second null should be searched by the optimization problem depends on the selected approach for handling the heat exhaust power. However, the main goal of our work was not to increase the wetted divertor surface (we agree with the Reviewer that in this case the additional null point should be placed near to the divertor (vertical) targets) neither the objective function was the position of the secondary x-point. Indeed, HFE experiments at JET, existing machine with fixed geometry wall, have been motivated by the aim to study the effects of flux expansion variation, mainly at the x-point location than at targets, on radiation fraction and divertor radiated power re-distribution. In the past at JET, with the MkI divertor, a systematic study of the influence of X-point height and poloidal flux expansion has been set up [C. Lowry , et al. , Divertor configuration studies on jet, J. Nucl. Mater. 241–243 (1997) 438–443, A. Loarte, et al., Plasma detachment in JET mark i divertor experiments, Nucl. Fusion 38 (3) (1998) 331–371] showing minor differences in the radiation distribution, whereas in [R. Pitts, et al., Divertor geometry effects on detachment in TCV, J. Nucl. Mater. 290–293 (2001) 940–946, doi: 10.1016/S0022-3115(00)00461-X] experiments and simulations have shown enhancement of detachment as the flux expansion was increased. More recently at JET, equipped with the ITER-like Wall (ILW), radiative seeded scenarios have been studied and only a maximum radiation fraction 75% has been achieved [M. Wischmeier, et al., Impurity Seeding on JET to Achieve Power Plant like Divertor Conditions, presented at 25th FEC – IAEA Conference, St Petersburg (2014), *http://www-naweb.iaea.org/napc/physics/FEC/FEC2014/fec2014-slides/94_EX72.pdf]. Indeed, high flux expansion configuration are predicted to increase the radiation in the vicinity of the X-point and have a ionization front extending further in the SOL than the LFE equilibrium, as discussed in [B. Viola et al., Nuclear Materials and Energy, 12 (2017) 786-790] and show here in Figure 1,2 – R2. Finally, HFE cases do seem to offer a benefit in reducing the nitrogen concentration needed to obtain a given radiated power level. As discussed in the paper the HFE experiments have shown that the flux expansion has effect on divertor radiation and on the movement of the radiation (nitrogen) front toward the primary x-point. However, no further increase of the Xpoint flux expansion has been obtained due to the technological restrictions on the polarity of the divertor coils. A further increase of both outer xpoint and target flux expansion, that is consequently translated into a movement variation for the secondary x2 xpoint from the inner to the outer divertor region, could be obtained by varying the polarity on D4 coil. However, only a brief discussion on experimental effect of flux expansion on radiation fraction will be given in the proposed paper because a contribution to the coming IAEA 2018 conference is already planned, mainly focused on the physical aspects of the HFE experiments.*

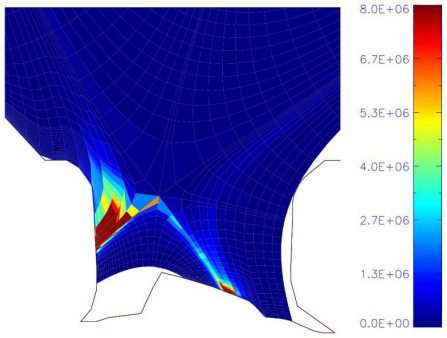

Figure 1-R2 Divertor radiated power (MW/m^3) from EDGE2D simulation for N2 seeded H-mode LFE discharge

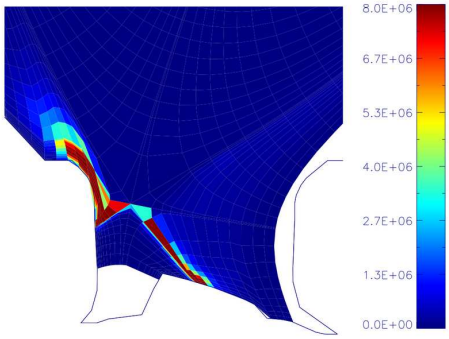

Figure 2-R2 Divertor radiated power (MW) from EDGE2D simulation for N2 seeded H-mode HFE discharge

Reviewer's comment #3: Moreover, in fig. 2C, the radiating region seems to invade the region where some divertor coils are allocated. Is this true? If this is the case, the authors should explain if this is acceptable? Anyway, the geometry of the divertor targets and coils should appear in fig. 2c.

Authors' reply:

We thank the Reviewer for the comments. The radiated power region due to nitrogen seeding is limited to the plasma region enclosed in the first wall. We have modified Fig.2b and Fig.2c in order to include the divertor targets and coils geometry.

Reviewer's comment #4: Additional remarks

a) Chapter 1. Introduction, Row 8: itself and its and its spatial derivatives -> itself and its spatial derivatives;

Authors' reply: *the typo has been corrected as suggested by the Reviewer.*

b) Chapter 3 Table I and following text. The flux expansion and dx1-x2 aren't adimensional quantities.

Authors' reply: *we have detailed in the aforementioned "authors replies" the definitions used for the flux expansion. In addition we have to mention that the distance d_x1_x2 is a normalized length. Indeed, in the new version of the paper we have added more details in the definition of dx1_x2 distance, now named as σ parameter, as following:*

➔ *Section 3: "…The distance between the two null-points, i.e the proximity to the exact SF [D.D. Ryutov, V.A. Soukhanovskii, Physics of Plasmas 22, 110901 (2015), G. Calabrò, et al., Nuclear Fusion 55 (8), 083005 (2015)], is parametrized here by the dimensionless factor σ = D/a, where D is the null-points separation distance and a is the plasma minor radius. SF like configuration corresponds to σ close to zero. The mutual position of the primary and secondary null-points determines the local geometry of the null region and hence the properties of the divertor. Experimental values of the flux expansion at the inner and outer x-point $f_{x,xp}$ vs. SF proximity parameter σ are shown in Fig. 4 for JET–ILW discharges. Both inner and outer $f_{x,xp}$ increase when moving from LFE (σ=1) to HFE configuration (0.25<σ<0.45). The maximum flux expansion increase has been obtained for the discharge #92086 by relaxing the plasma distance to the inner wall. It should be noted that this configuration cannot be used in H-mode discharges because of the limitations on the permitted operational plasma-wall distance for heated plasmas."*

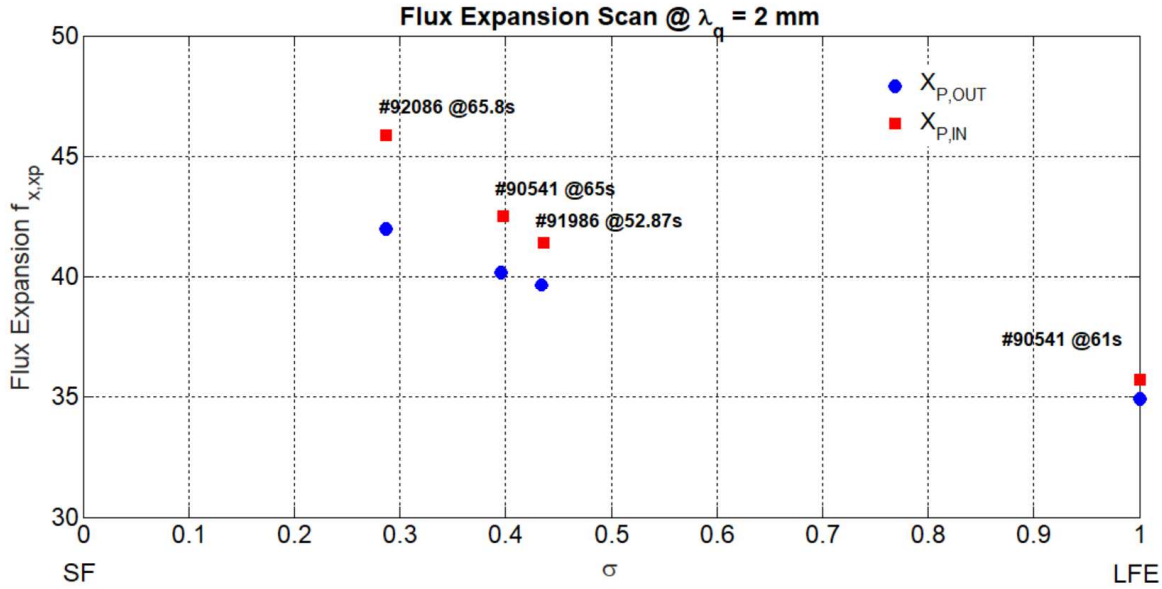

(New) Figure 4. Experimental variations of the flux expansion at the inner and outer xpoint $f_{x,xp}$ Vs. SF proximity parameter σ. Both inner and outer $f_{x,xp}$ increase when moving from LFE configuration (σ=1) to HFE configuration (0.25<σ<0.45), characterized by the presence of 2-nearby poloidal field nulls.

c) Chapter 3 Fig.2: In Figg. 2b and 2c, the topology of the plasma is superposed with the iso-module lines. This could generate confusion. In the legend: "magnetic field topology, shown as magenta iso-lines" -> "magnetic field module, shown as magenta iso-lines". In Fig.3 the vertical axis is adimensional.

***Authors' reply**: the typo has been corrected as suggested by the Reviewer. In addition we have modified the Fig.2b) and 2c) as following:*

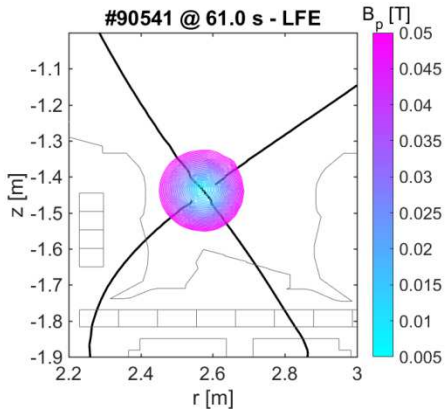

(New) Fig.2b. *Plasma separatrix and poloidal magnetic field module iso-lines, with B_P varying from 0-0.05T, are shown for LFE configuration.*

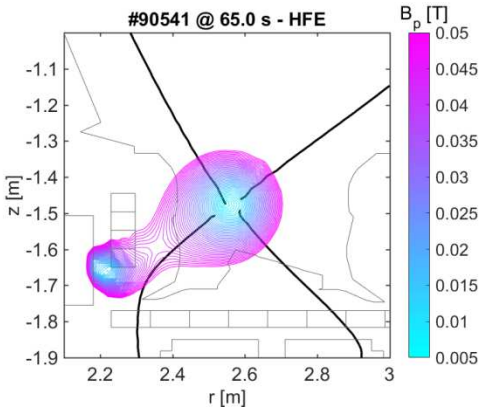

(New) Fig.2c. *Plasma separatrix and poloidal magnetic field module iso-lines, with B_P varying from 0-0.05T, are shown for LFE configuration.*

d) Chapter 4 . Conclusion. Row 4: On the high filed side, -> on the high field side

***Authors' reply**: the typo has been corrected as suggested by the Reviewer.*

Divertor currents optimization procedure for JET-ILW high flux expansion experiments

G. Calabrò[a], F. Maviglia[b], S. Minucci[a], B. Viola[c] and JET Contributors[*]

[a]*Department of Economics, Engineering, Society and Business Organization (DEIm), University of Tuscia, Largo dell'Università snc, 01100 Viterbo, Italy*
[b]*Consorzio CREATE, via Claudio 21, 80125, Napoli, Italy*
[c]*ENEA for EUROfusion, via E. Fermi 45, 00044 Frascati (Roma), Italy.*

simone.minucci@unitus.it

Abstract. This paper deals with a divertor coil currents optimized procedure to design High Flux Expansion (HFE) configurations in the JET tokamak aimed to study the effects of flux expansion variation on the radiation fraction and radiated power re-distribution. A number of benefits of HFE configuration have been experimentally demonstrated on TCV, EAST, NSTX and DIII-D tokamaks and are under investigation for next generation devices, as DEMO and DTT. The procedure proposed here exploits the linearized relation between the plasma-wall gaps and the Poloidal Field (PF) coil currents. Once the linearized model is provided by means of CREATE-NL code, the divertor coils currents are calculated using a constrained quadratic programming optimization procedure, in order to achieve HFE configuration. Flux expanded configurations have been experimentally realized both in ohmic and heated plasma with and without nitrogen seeding. Preliminary results on the effects of the flux expansion variation on total power radiation increase will be also briefly discussed.

Keywords: Advanced Configuration, Quadratic Programming Optimization, Flux Expansion, Scrape-Off Layer

1. Introduction

Heat and particle loads on the plasma facing components are among the most challenging issues to be solved to design a nuclear fusion reactor [1, 2]. An approach to handle the heat exhaust power is to use alternative magnetic configurations, such as Snowflake Divertor (SF) [3] and recently described divertor with a strong flux flaring in a single divertor leg [4, 5]. Such a configuration places the second x-point near the plate, causing flared field lines in that region which spread the heat load over a larger area and increase the line connection length. Recently, a number of additional benefits of High Flux Expansion (HFE) configurations have been experimentally demonstrated on TCV [6] and DIII-D [7]. On the former, HFE configuration showed deeper detachment and a reduction of the radiation location sensitivity with respect to the plasma core density, with increasing flux expansion and flaring; on the latter, it showed that increasing flux expansion and flaring allow for detachment at lower density and higher pedestal pressure. Nevertheless, the SF configuration is characterized by a second-order null (x-point) in the poloidal magnetic field (B_P), where both B_P itself and its spatial derivatives vanish. This splits the separatrix in the nearness of the null into six segments: two of them enclose the confined plasma and the others lead to the machine wall (the divertor legs). The poloidal cross-section of the obtained magnetic flux surfaces with a hexagonal null-point resembles a snowflake. Theoretical studies indicate that the SF magnetic geometry may lead to both higher power losses during Scrape-Off Layer (SOL) transport and an increased plasma wetted area of the wall [8]. As it was realized in the first assessment of the SF [3], an exact SF configuration is topologically unstable: any plasma perturbation or imbalance of the Poloidal Field (PF) coils current splits the second-order null into two first-order nulls, leading to a variety of topologically-stable SF-like configurations [8]. The secondary null can be moved around to change its distance from the first one and to form a magnetic configuration that features either a contracting or a flaring geometry near the plate [3-5, 8]. The linear dependence of the gradient of magnetic field B_P in the primary null with respect to distance between the two nulls is described in [9, 10] and characterizes the interdependence of the field structures of both nulls. This feature will be analyzed for JET: the flaring of the magnetic flux (characterized by the magnetic field gradient) in the primary null is affected by the presence of the

[*]See the author list of X. Litaudon et al 2017 Nucl. Fusion 57 102001

secondary null. This flaring is then directly translated in the increased wetted surface area and reduced heat flux [5, 8] or in a total radiated power increase, as it will be discussed in the paper.

In the past at JET, with the MkI divertor, a systematic study of the influence of x-point height and poloidal flux expansion has been set up [11, 12] showing minor differences in the radiation distribution, whereas in [4], experiments and simulations have shown an enhancement of detachment as the flux expansion was increased. More recently at JET, equipped with ITER-like Wall [13], radiative seeded scenarios have been studied and only a maximum 75% radiation fraction has been achieved [14]. However, recent predictive studies [15] have shown that HFE configurations increase the radiation in the proximity of the x-point and have an ionization front extending further in the Scrape-Off Layer (SOL) than in the Low Flux Expansion (LFE) case. In addition, HFE cases do seem to offer a benefit in reducing the nitrogen concentration needed to obtain a given radiated power level [15]. Here, we will discuss the modelling, creation and control of HFE configurations at JET–ILW, characterized by the presence of two nearby poloidal field nulls in the divertor region, aimed to study the effects of flux expansion variation on radiation fraction and radiated power re-distribution.

The paper is organized as follows: Section 2 describes the HFE configuration design and optimization, taking into account the technological constraints of JET tokamak. In Section 3, preliminary experimental results of ohmic, nitrogen seeded high confinement (H-mode) HFE, and LFE discharges will be discussed, supported by interpretative 2D edge modelling. Finally, Section 4 draws the main conclusions and outlook.

2. Constrained optimization procedure

The JET tokamak has eight PF coils potentially useful for plasma shape control (see Fig. 1) and are denoted by $P_1 \ldots P_4$ and $D_1 \ldots D_4$. The P-coils are not equipped with their own power supply but are connected each other and fed by five circuits [10]. The currents flowing in these circuits are denoted by I_{P1E}, I_{PFX}, I_{SHA}, I_{P4T}, I_{P4I}, whereas each divertor coil (D-coils) is fed by its own power supply that sustain a current denoted by I_{Di}, with $i = 1 \ldots 4$. Therefore, nine circuits are available to the plasma control system. The circuit P_{1E} is used to control the plasma current, whereas the other eight circuits are used to control the plasma shape.

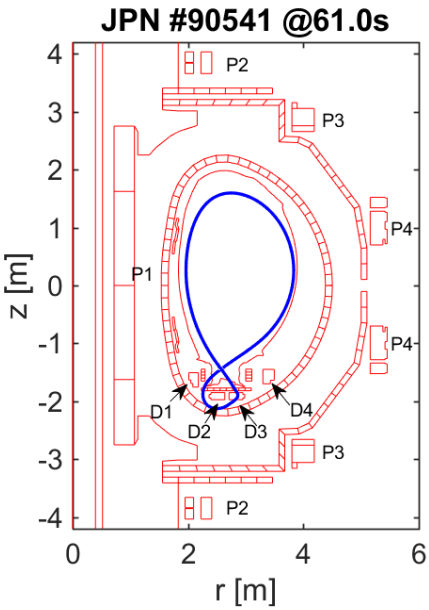

Figure 1. Cross section of the JET tokamak. The plasma boundary of the JET discharge #90541 at 61s is shown in blue. The poloidal coils (P1–P4 and D1–D4) and the toroidal coils, which surround the plasma ring, produce the required magnetic field for plasma confinement. Here, the D coils current are used in the optimization procedure in order to locally modify the magnetic topology in the divertor region.

The magnetic geometry in the divertor can be modified by changing the flux expansion at the target $f_{x,t} = dr_{target}/\lambda_q$ [16]: dr_{target} is the distance along the First Wall boundary between the inner (or outer) strike points of the separatrix and of the SOL boundary (i.e. the flux surface at one e-folding length power decay λ_q away from the separatrix); λ_q is the SOL width on the outer plane containing the plasma centroid. It should be noted that in JET, due to the location and geometry of the target plates, the inner and outer strike points of SOL boundary might be in a different position when moving from LFE to HFE configuration. In order to avoid this issue we consider the Full Flux Expansion at the target as the ratio between $dr_{target,tube}$ (i.e. the poloidal expansion of the magnetic flux tube at the target) and the SOL width (see Fig.2a in Section 3). In addition, we consider the flux expansion at x-point as $f_{x,xp} = dr_{xpoint}/\lambda_q$, where dr_{xpoint} is the Euclidian distance between the x-point and the SOL boundary along the horizontal line inward and outward the x-point height (see Fig.2a). For sake of consistency, the same rectangular grid has been used when scanning the SOL width on the plane containing the plasma centroid. Specifically, SOL width λ_q of 2, 5 and 10 mm have been considered. Here, HFE configuration characterized by the presence of 2-nearby divertor poloidal field nulls have been designed and optimized by means of CREATE-NL code (non-linear plasma evolution code), described in [17]. The procedure proposed for the design and optimization of the equilibria using the CREATE-NL code exploits the linearized relation between the plasma-wall gaps (the distance between the plasma surface and the first wall, measured along a given direction [18]) and the PF currents in two steps. The first step allows to have a first cut of the HFE equilibrium starting from a standard Single Null (SN) LFE configuration; a new equilibrium with a second null point within a limited distance from the LFE x-point is obtained, forcing the plasma boundary to be almost unchanged, apart from the region in the nearness of the null point. The second step refines the plasma shape and possibly reduces the PF coil currents while fulfilling the machine technological constraints. Once the linearized model is provided by means of CREATE-NL code, the divertor coils current needed to achieve the HFE configuration are calculated by means of a constrained quadratic programming optimization procedure [19, 20], generally stated as follows:

$$\min_{\underline{x}} \frac{1}{2} \underline{x}^T \underline{\underline{H}} \underline{x} + \underline{f}^T \underline{x} \text{ subject to: } \begin{cases} \underline{\underline{A}} \cdot \underline{x} = \underline{b} \\ \underline{l_b} \le \underline{x} \le \underline{u_b} \end{cases} \quad (1)$$

where the symmetric matrix $\underline{\underline{H}}$ represents the quadratic term, the vector $\underline{f}$ is the linear term, whilst the matrix $\underline{\underline{A}}$ and the vector $\underline{b}$ represent respectively the linear coefficients and the constant in the constraint of Eq. (1). At last, vectors $\underline{l_b}$ and $\underline{u_b}$ represent respectively the lower and upper bounds elementwise in (1). Once matrix $\underline{\underline{H}}$ and vector $\underline{f}$ are set up respectively as identity matrix and zero vector, finding a minimum for a problem specified by Eq. (1) turns into minimizing the Euclidean norm of the unknown vector $\underline{x}$ and guaranteeing the convexity of the objective function as well as the uniqueness of the optimization problem solution. Hence, Eq. (1) is adapted to the specific problem of achieving HFE plasma configurations while minimizing currents variation $\underline{\Delta I}$ in the PF coils subject to technological restrictions. Indeed, the vector $\underline{x} = \underline{\Delta I}$ must accomplish specific constraints, modelled by means of the linear equality constraints set thanks to the adopted linearized model: plasma shape and total plasma current are requested to be kept unchanged, whilst flux expansion is increased. Moreover $\underline{x}$ must be bounded according to the current restrictions on PF coil power supplies. Consequently, the constrained quadratic programming optimization procedure turns into the following problem:

$$\min \left\| \underline{\Delta I} \right\|_2 \text{ subject to: } \begin{cases} \underline{\underline{A}}_{gaps-I} \cdot \underline{\Delta I} = \underline{0} \\ \underline{L}^T_{plasma-I} \cdot \underline{\Delta I} = 0 \\ \underline{\underline{A}}_{FExp-I} \cdot \underline{\Delta I} = \underline{\delta}_{FExp} \\ \underline{I}_{\min} - \underline{I}_0 \le \underline{\Delta I} \le \underline{I}_{\max} - \underline{I}_0 \end{cases} \quad (2)$$

where:

- $\underline{\underline{A}}_{gaps-I}$ represents the linearized relationship between the I_{PF} currents and the plasma-wall gaps to be controlled (the first constraint states that the variation of I_{PF} currents does not affect the plasma-wall gaps); the following five gaps have been specifically considered [17] in our analyses: Radial Outer Gap (ROG), Radial Inner Gap (RIG), Top Gap (TOG), R coordinate of Outer Strike Point (RSOGB) and Z coordinate of Inner Strike Point (ZSIGB);
- $\underline{L}_{plasma-I}$ represents the mutual inductance vector between the plasma and the active coils (the second constraint states that the variation of I_{PF} currents does not affect the total plasma current);
- $\underline{\underline{A}}_{FExp-I}$ represents the linearized relationship between the I_{PF} currents and the magnetic flux expansion (the third constraint states that the variation of I_{PF} currents changes the flux expansion, here assumed to be the Full flux Expansion $f_{x,t}$ of the SOL boundary with decay length λ_q = 2mm, according to $\underline{\delta}_{FExp}$).
- $\underline{I}_0$ is the I_{PF} currents vector in the reference equilibrium (the last constraint bounds the currents flowing into the I_{PF} currents according to the technological restrictions of each power supply, in terms of minimum and maximum attainable values; specifically, the following lower and upper bounds have been considered for each of the divertor coil: I_{D1}{0,19kA}, I_{D2}{0,37kA}, I_{D3}{0,37kA}, I_{D4}{-18kA,0}.

It should be noted that the upper and lower current bounds are additionally constrained by the power supplies topology and in particular by the AC-DC converters [17]. In particular, they are two voltage quadrants rectifiers, able to change the polarity of the only voltage across their terminals, whilst the current polarity can be changed only by means of a switch that inverts the taps of the coils. For this reason, the poloidal currents can range only in one quadrant of the current-voltage operating plane, adding an additional constraint for the optimization problem. In the experiments discussed hereafter, the maximum attainable flux expansion has been mainly limited by the polarity of the D-coils (positive for I_{D1},..I_{D3} and negative for I_{D4}) and in particular by that of D4 coil. As discussed in [21], an increase of the flux expansion could be achieved by changing the polarity on D2 and D4 coils.

3. Experimental results

Initial HFE ohmic and nitrogen seeded H-mode discharges, at plasma current I_P=1.8MA have been successfully achieved at JET – ILW. Table I reports the values of both $f_{x,t}$ and $f_{x,xp}$, considering a SOL width of λ_q=2mm, for the ohmic discharge #90541 when moving from LFE to HFE configuration. Plasma separatrix and flux surface at λ_q=1cm for both LFE and HFE configurations are shown in Fig. 2a. Plasma separatrix and poloidal magnetic field module iso-lines, with B_P varying from 0-0.05T, are shown for both LFE (Fig. 2b) and HFE (Fig.2c) configurations. It should be noted that the magnetic field flatness region is increased for HFE configuration thanks to the presence of a second x-point.

Table I. Flux expansion on inner and outer x-point plane and targets. A SOL width of λ_q = 2 mm has been considered, accordingly with the length-decay of the thermal power in the SOL in JET tokamak [2].

	$f_{x,xp/IN}$	$f_{x,xp/OUT}$	$f_{x,t/IN}$	$f_{x,t/OUT}$
HFE JPN #90541 @ 65 s I_{D1} = 6.36 kA, I_{D2} = 5.04 kA, I_{D3} = 11.19 kA, I_{D4} = 0 kA	42.52	40.44	12.63	5.96
LFE JPN #90541 @ 61 s I_{D1} = 1.51 kA, I_{D2} = 13.91 kA, I_{D3} = 6.41 kA, I_{D4} = -4.34 kA	35.66	34.39	6.20	4.08

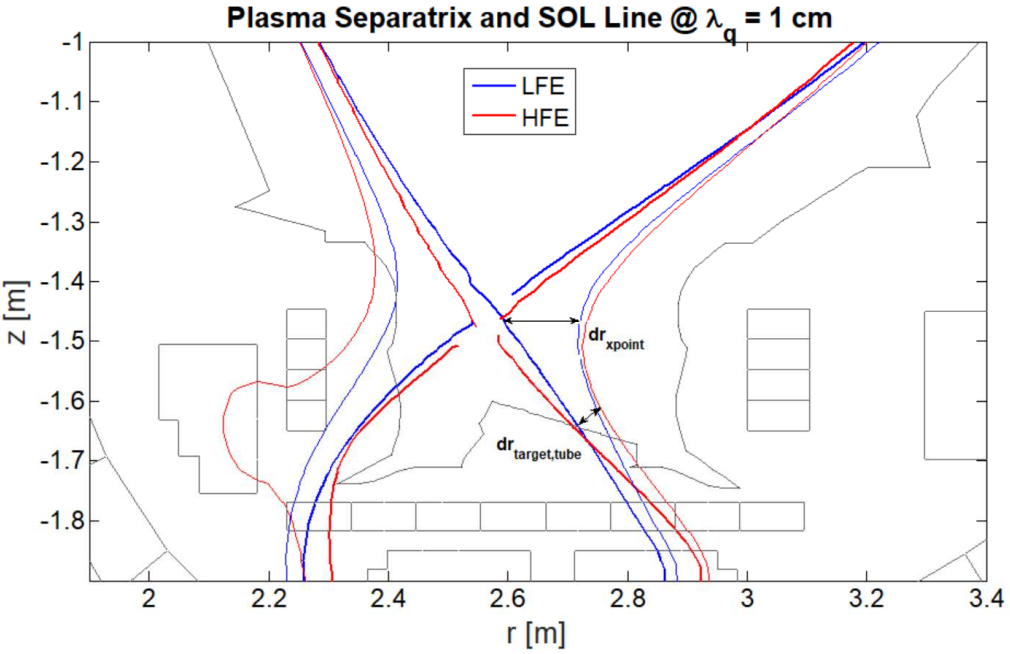

a)

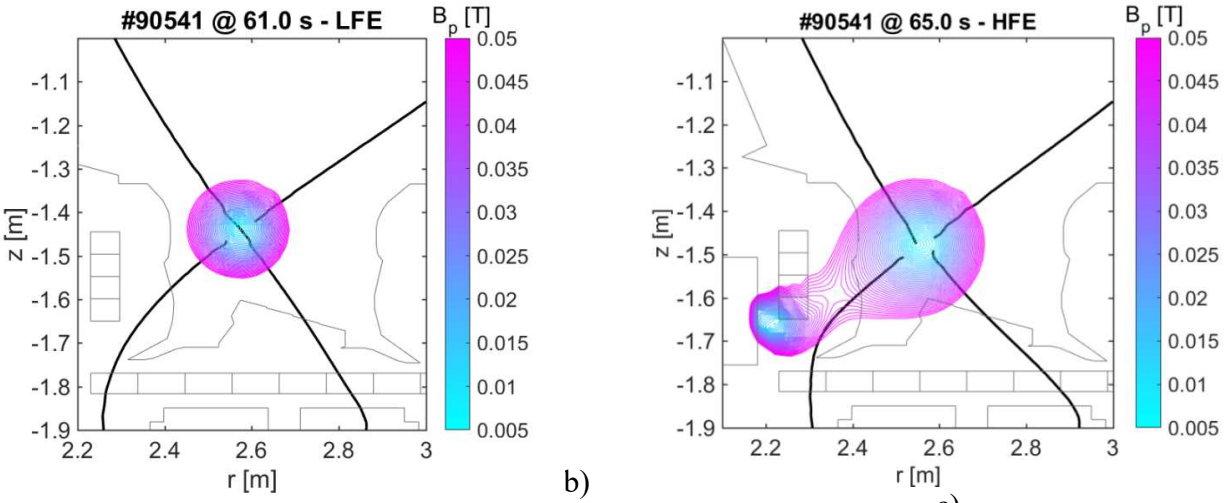

b) c)

Figure 2. a) Plasma separatrix and SOL flux surface with λ_q=1cm, for both LFE (blue solid lines for discharge #90541 at 61s) and HFE (red solid line for discharge #90541 at 65s) configurations; Plasma separatrix (black solid line) and poloidal magnetic field module iso-lines, with B_P varying from 0-0.05T, are shown for both LFE (b) and HFE (c) configurations.

An experimental flux expansion increase by a factor of ~20% at primary x-point inwards and ~50% on the outer divertor target has been achieved, thanks to the generation of a second null point close to inner part of the first wall. Fig. 3 shows a comparison between experimental LFE (blue color) and HFE configuration (red color) in terms of plasma-wall gaps (i.e. ROG, RIG, TOG, RSOGB and ZSIGB), plasma current I_P and divertor coils current needed to increase the flux expansion. The distance between the two null-points, i.e the proximity to the exact SF [9, 10], is parametrized here by the dimensionless factor $\sigma = D/a$, where D is the null-points separation distance and a is the plasma minor radius. SF like configuration corresponds to σ close to zero. The mutual position of the primary and secondary null-points determines the local geometry of the null region and hence the properties of the divertor. Experimental values of the flux expansion at the inner and outer x-point $f_{x,xp}$ vs. SF proximity parameter σ are shown in Fig. 4 for JET–ILW discharges. Both inner and outer $f_{x,xp}$ increase when moving from LFE ($\sigma=1$) to HFE configuration ($0.25<\sigma<0.45$). The maximum flux expansion increase has been obtained for the discharge #92086 by relaxing the plasma distance to the inner wall. It should be noted that this configuration cannot be used in H-mode discharges because of the limitations on the permitted operational plasma-wall distance for heated plasmas.

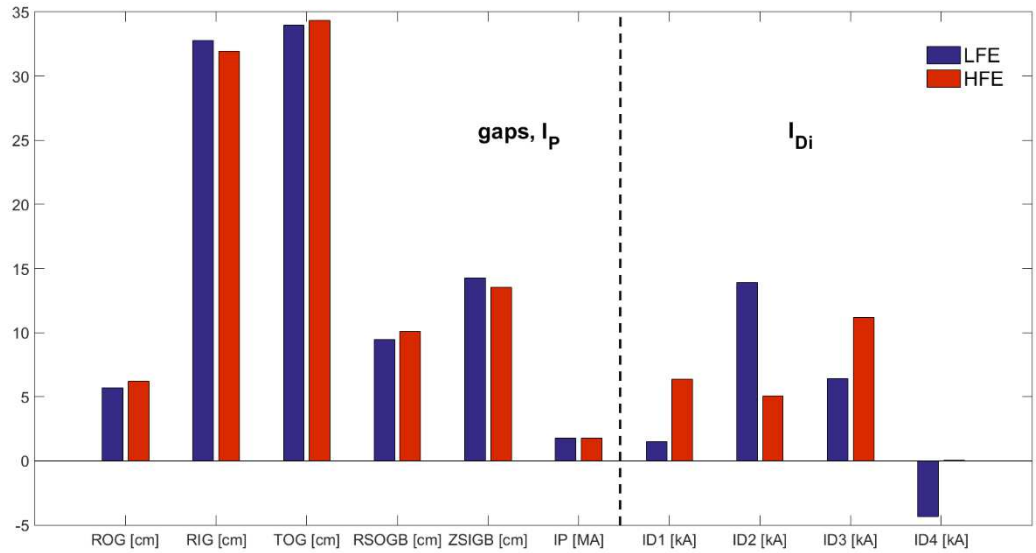

Figure 3: Comparison between experimental LFE (blue color) and HFE configuration (red color) in terms of gaps (i.e. ROG, RIG, TOG, RSOGB and ZSIGB) and plasma current I_P, to be kept almost unchanged according to Eq.(2), and divertor coil currents needed to increase the flux expansion. The maximum attainable flux expansion has been mainly limited by the polarity on D4 coil.

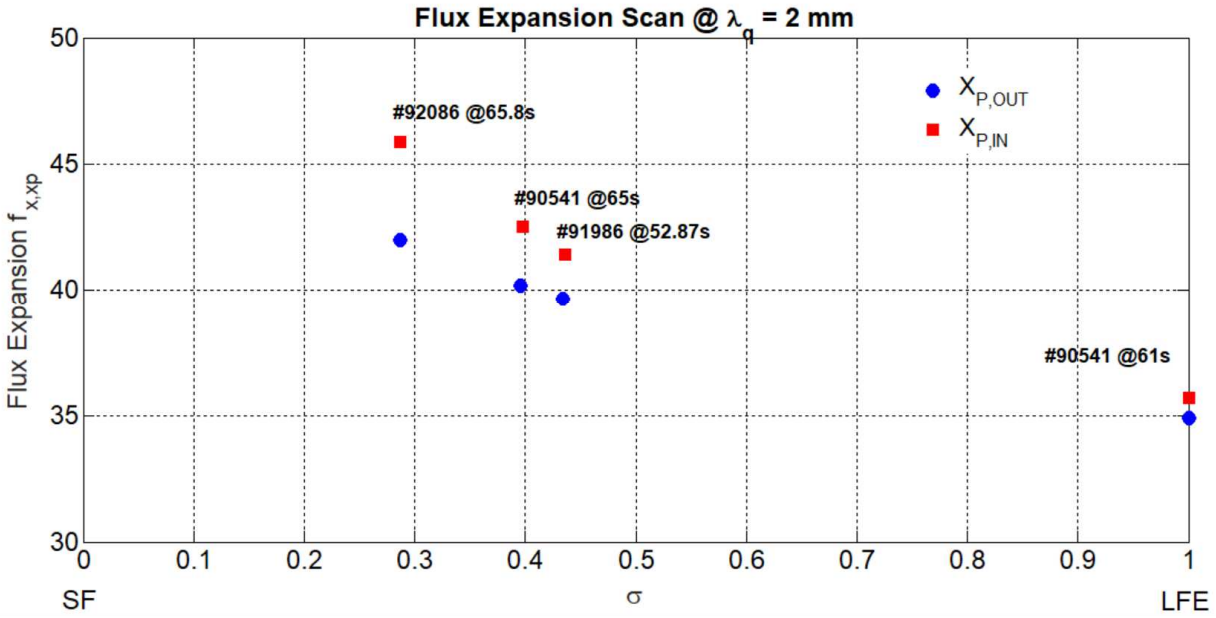

Figure 4. Experimental values of the flux expansion at the inner and outer x-point $f_{x,xp}$ vs. SF proximity parameter σ. Both inner and outer $f_{x,xp}$ increase when moving from LFE configuration (σ=1) to HFE configuration (0.25<σ<0.45), characterized by the presence of 2-nearby poloidal field nulls.

Finally, the aforementioned LFE and HFE configurations have been recently used to address the physics of a possible dependence of radiative volume and total radiated power on the distance between the two nulls [15]. Aim of this study has been the evaluation of the impact of main magnetic divertor geometry parameters, as the flux expansion and the connection length, on the radiation pattern disentangled by the change of recycling happening at the same time, focusing on bolometer and Langmuir probe measurements analysis supported by EDGE2D-EIRENE code [22-23] interpretative modelling. A detailed analysis of the power balance has been set up, as well discussed in [15], to physically investigate the reason of the increase of the radiated power for HFE discharges. In summary, although the nitrogen radiation is constant in all the studied cases, the increase of 20% of the total radiation power in the high flux expansion case does mainly seem due to the molecular and charge exchange losses. As discussed in [15], an increase of charge exchange losses has been related to an increase of connection length and flux expansion both at x-point at strike points position.

4. Conclusions

The demonstration of the possibility of creating and controlling a two nearby poloidal field nulls in JET-ILW tokamak has been achieved, showing an increase on magnetic poloidal flux expansion both at x-point and strike points position. Initial experiments with a second null, located in the proximity of the inner divertor region have been performed, forming a configuration with significant distance between the two nulls and a contracting geometry near the target plates, leading to an increase of the main magnetic divertor geometry parameters. In addition, preliminary nitrogen seeded H-mode experiments have been set-up showing an increase of the total radiated power of the same factor of the flux expansion increase. Further experiments will be devoted to change the divertor coils polarities in order to move the secondary null point on the outer divertor region and consequently increase the outer x-point and target flux expansion.

Acknowledgments

The authors would like Prof. R. Albanese, Dr. F. Crisanti and Dr. G. Artaserse for their fruitful suggestions. This work has been carried out within the framework of the EUROfusion Consortium and has received funding from the Euratom research and training programme 2014-2018 under

grant agreement No 633053. The views and opinions expressed herein do not necessarily reflect those of the European Commission.

References

[1] A. Loarte et al., Chapter 4: Power and particle control, in: *Nuclear Fusion*, 47 (6), pp. S203
[2] Team Asdex Upgrade, T. Eich, B. Sieglin, A. Scarabosio, W. Fundamenski, R. J. Goldston, A. Herrmann, Inter-ELM power decay length for JET and ASDEX Upgrade: measurement and comparison with heuristic drift-based model, *Physical Review Letters*, 107 (21), 215001 (2011)
[3] D. D. Ryutov, Geometrical properties of a "snowflake" divertor, *Physics of Plasmas*, *14* (6), 064502 (2007)
[4] R. A. Pitts, B. P. Duval, A. Loarte, J. M. Moret, J. A. Boedo, D. Coster, I. Furno, J. Horacek, A. S. Kukushkin, D. Reiter, J. Rommers, Divertor geometry effects on detachment in TCV, *Journal of Nuclear Materials*, 290-293, 940-946 (2001)
[5] M. Kotschenreuther, P. Valanju, B. Covele, S. Mahajan, Magnetic geometry and physics of advanced divertors: The X-divertor and the snowflake, *Physics of Plasmas*, 20 (10), 102507 (2013)
[6] C. Theiler et al., Results from recent detachment experiments in alternative divertor configurations on TCV, *Nuclear Fusion*, *57*(7), 072008 (2017)
[7] B. M. Covele, M. Kotschenreuther, S. Mahajan, P. Valanju, A. Leonard, J. Watkins, M. Makowski, M. Fenstermacher, H. Si, Increased heat dissipation with the X-Divertor geometry facilitating detachment onset at lower density in DIII-D, *Nuclear Fusion*, 57, 8 086017, (2017)
[8] D. D. Ryutov, M. A. Makowski, M. V. Umansky, Local properties of the magnetic field in a snowflake divertor, *Plasma Physics and Controlled Fusion*, 52 (10), 105001 (2010)
[9] D. D. Ryutov, V. A. Soukhanovskii, The snowflake divertor, *Physics of Plasmas*, 22 (11), 110901 (2015)
[10] G. Calabrò et al., EAST alternative magnetic configurations: modelling and first experiments, *Nuclear Fusion*, 55 (8), 083005 (2015)
[11] C.G. Lowry et al., Divertor configuration studies on JET, *Journal of Nuclear Materials*, 241–243, 438-443, ISSN 0022-3115, https://doi.org/10.1016/S0022-3115(97)80078-5 (1997).
[12] A. Loarte et al., Plasma detachment in JET Mark I divertor experiments, *Nuclear Fusion*, 38 (3), 331-371 (1998)
[13] E. Joffrin et al., First scenario development with the JET new ITER-like wall, *Nuclear fusion*, 54 (1), 013011 (2013).
[14] C. Lowry, M. Wischmeier, A. Huber, C. F. Maggi, K. McCormick, M. Reinke, et al., Impurity Seeding on JET to Achieve Power Plant Like Divertor Conditions, presented at *25th IAEA Fusion Energy Conference* (FEC 2014), Saint Petersburg, 13-18/10/2014.
[15] B. Viola, G. Calabró, A. E. Jaervinen, I. Lupelli, F. Maviglia, S. Wiesen, M. Wischmeier and JET Contributors, EDGE2D-EIRENE simulations of the impact of poloidal flux expansion on the radiative divertor performance in JET, *Nuclear Materials and Energy*, 12, 786-790 (2017)
[16] H. Reimerdes et al., TCV experiments towards the development of a plasma exhaust solution, *Nuclear Fusion*, 57 (12), 126007 (2017)
[17] R. Albanese, R. Ambrosino, M. Mattei, CREATE-NL+: A robust control-oriented free boundary dynamic plasma equilibrium solver, *Fusion Engineering and Design*, 96, 664-667 (2015)
[18] M. Ariola, A. Pironti, Magnetic Control of Tokamak Plasmas, Advances in Industrial Control, Vol. 187, Springer-Verlag, London (2008)

[19] T. F. Coleman, Y. Li, A reflective Newton method for minimizing a quadratic function subject to bounds on some of the variables, *SIAM Journal on Optimization*, 6 (4), 1040–1058 (1996)
[20] N. Gould, P. L. Toint, Preprocessing for quadratic programming, *Mathematical Programming*, 100 (1), 95–132 (2004)
[21] Calabrò, G. et al., Divertor configuration with two nearby poloidal field nulls: modelling and experiments for EAST and JET tokamaks, presented at *22nd International Conference on Plasma Surface Interactions in Controlled Fusion Devices (PSI 22)* Rome, 30/05-03/06/2016
[22] R. Simonini, G. Corrigan, G. Radford, J. Spence, A. Taroni, Models and Numerics in the Multi-Fluid 2-D Edge Plasma Code EDGE2D/U, *Contributions to Plasma Physics*, 34 (2-3), 368-373 (1994)
[23] S. Wiesen, EDGE2D/EIRENE code interface report, Technical Report Online available: http://www.eirene.de/e2deir_report_30jun06.pdf (2006)